Cholesterol Crystal Nucleation from Enzymatically Modified Low-Density Lipoproteins: Combined Effect of Sphingomyelinase and Cholesterol Esterase[†]

Andrew J. Guarino,[‡] Thomas N. Tulenko,[§] and Steven P. Wrenn*,[‡]

Chemical Engineering Department, Drexel University, 3141 Chestnut Street, CAT Building, Philadelphia, Pennsylvania 19104, and Department of Surgery, Thomas Jefferson University, Philadelphia, Pennsylvania 19106

Received September 26, 2003; Revised Manuscript Received December 3, 2003

ABSTRACT: An assay detecting and quantifying cholesterol nucleation from low-density lipoproteins has been established. Förster resonance energy transfer between dehydroergosterol and dansylated lecithin becomes significantly alleviated as a consequence of conucleation of dehydroergosterol and cholesterol. The assay, in combination with dynamic light scattering, absorbance spectroscopy, and fluorescence microscopy, can be used to study aggregation and nucleation in model blood systems. Human plasma LDL was labeled with dehydroergosterol and dansylated lecithin by incubation with donor multilamellar liposomes and isolated by centrifugation. Exposure of labeled LDL (0.5 mg/mL of total lipids) to sphingomyelinase (0.0−0.2 unit/mL) led to modest particle aggregation but produced no changes in energy transfer and no crystallization. However, addition of sphingomyelinase produced significant particle aggregation, nucleation, and crystallization, in a dose-dependent fashion, in samples that were previously treated with the enzyme, cholesterol esterase (0.2 unit/mL). The combination of cholesterol esterase and sphingomyelinase led to a significant alleviation of energy transfer, which preceded by 24 h the appearance of fluorescent, microscopic sterol crystals. These results point to a synergistic effect between cholesterol esterase and sphingomyelinase, suggesting that mere aggregation of LDL is insufficient to promote nucleation, and crystal formation likely proceeds in the intracellular space after LDL uptake by macrophages.

Cholesterol (Chol)[1] crystals are recognized as a hallmark of advanced atherosclerotic plaques (*1*). Numerous studies confirm the existence of cholesterol monohydrate crystals, which are presumed to play an important role in cell disruption and necrosis, within the lipid core of plaques (*2*). Moreover, recent studies point to the importance of crystalline cholesterol as a determinant of plaque morphology (*3*), which has been demonstrated to be directly related to the incidence of plaque rupture and thrombosis (*4*). Given that stable plaques are relatively benign and myocardial infarction requires thrombosis-driven occlusion of an artery triggered by plaque rupture (*5*), the formation of cholesterol crystals in atherosclerosis is an important, but poorly understood, issue in vascular biology that needs to be addressed.

Cholesterol crystals nucleate in the lipid core because the concentration of free cholesterol there exceeds its solubility limit. The crystals, which are inert, form sequential layers in which newly deposited crystals enter from the luminal side of the lesion (*1*). However, the origin of the crystals within the lipid core and the mechanism by which they nucleate are largely unknown. Several studies indicate that the crystals originate from intracellular lipid accumulated by foam cells (*6*), while others suggest that the crystals originate from extracellular lipid that is trapped within the lesion (*7*). While useful, these studies utilize crystal detection methods (for example, microscopy) that are at best semiquantitative and do not provide molecular information concerning the cholesterol nucleation event.

Nucleation of cholesterol crystals necessarily involves clustering of cholesterol molecules to exceed a critical cluster size or nucleus. Recent evidence suggests that cholesterol clustering takes place within a lipid membrane and that cholesterol laterally phase separates within a membrane, yielding discrete cholesterol domains, prior to macroscopic precipitation (*8*). In undersaturated systems [that is, a cholesterol mole fraction less than 0.66 for phosphatidylcholine (PC) membranes] (*9*), cholesterol domains are thermodynamically stable. However, in supersaturated systems the domains are metastable and ultimately precipitate from the membrane. The process of nucleation continually removes cholesterol from the membrane and delivers cholesterol to the nascent crystalline phase, which grows and eventually produces macroscopic cholesterol monohydrate crystals. An analytical method that is sensitive to this separation of cholesterol from the phospholipid's membrane offers the possibility of measuring the molecular events associated with cholesterol nucleation.

[†] This work was supported in part by a Biomedical Engineering Research Grant from The Whitaker Foundation and by an ARA Award to S.P.W. sponsored by Pfizer, Inc.

* To whom correspondence should be addressed. Phone: (215) 895-6694. Fax: (215) 895-5837. E-mail: wrenn@coe.drexel.edu.

[‡] Drexel University.

[§] Thomas Jefferson University.

[1] Abbreviations: FRET, Förster resonance energy transfer; DHE, dehydroergosterol; DL, 1-acyl-2-[12-[(5-(dimethylamino)-1-naphthalenesulfonyl)amino]dodecanoyl]-*sn*-glycero-3-phosphocholine; LDL, low-density lipoprotein; SMase, sphingomyelinase; CEase, cholesterol esterase; R_F, fluorescence ratio; DLS, dynamic light scattering; PLC, phospholipase C; Chol, cholesterol; egg PC, egg lecithin; PC, phosphatidylcholine; SM, egg sphingomyelin; MLVs, multilamellar vesicles.

10.1021/bi035747r CCC: $27.50
Published on Web 01/22/2004

An ideal candidate is fluorescence energy transfer from dehydroergosterol (DHE) to dansylated lecithin (DL), which are fluorescent analogues of the native lipids cholesterol and phospholipids, respectively. We recently developed an assay for cholesterol nucleation based on DHE-to-DL energy transfer, which takes advantage of the fact that the efficiency of energy transfer depends heavily ($1/r^6$) on the separation, r, between fluorophores (*10*). The efficiency of energy transfer is relatively high when both fluorophores are in the membrane, resulting in a small ratio of (DHE-to-DL) fluorescence intensities. Nucleation of DHE, which has been shown to cocrystallize with cholesterol (*11*), into the nascent crystalline phase alleviates energy transfer due to an increase in distance between nucleated DHE and DL remaining in the membrane. This leads to a measurable increase in the (DHE-to-DL) ratio of fluorescence intensities, which is used to quantify the extent and rate of cholesterol nucleation.

We have used the DHE-to-DL energy transfer to characterize cholesterol nucleation from lecithin−cholesterol vesicles in the presence of the proaggregating enzyme, PLC (*12*). More recently, we used the assay to study nucleation from vesicles upon exposure to the bile salt, sodium taurocholate (*13*). An interesting result of that work was the observation of what appears to be equilibrium, laterally phase-separated cholesterol domains within the vesicle bilayer (*8*). These cholesterol domains, which have also been reported in membranes derived from smooth muscle cells (*14*), are possible precursors to macroscopic cholesterol crystals. Others have used the assay to examine the kinetics and mechanism of transbilayer movement of sterols (*15*).

Here we demonstrate that the DHE-to-DL energy transfer methodology can be adapted to low-density lipoprotein-(LDL-) based systems so as to examine cholesterol nucleation in the context of atherosclerosis. We show that neither of the enzymes, sphingomyelinase (SMase) or cholesterol esterase (CEase), alone promotes cholesterol nucleation but that these two enzymes act together to facilitate rapid cholesterol nucleation in vitro. SMase is an enzyme that is present in the arteries and widely accepted to contribute to atherosclerosis via aggregation, and subsequent retention, of LDL. Indeed, LDL aggregation and retention is thought to be the "central pathogenic process in atherosclerosis" (*16, 17*) as described by the response-to-retention hypothesis. CEase is an intracellular enzyme that hydrolyzes esterified cholesterol to free cholesterol. As esterified cholesterol does not crystallize and its conversion to free cholesterol increases the level of supersaturation, CEase is considered an important contributor to cholesterol nucleation in the context of atherosclerosis (*18*).

MATERIALS AND METHODS

Materials. Cholesterol (Chol), egg lecithin (egg PC), DHE, and sphingomyelinase (SMase) from *Bacillus cereus* (<1% PLC activity) were all purchased from Sigma (St. Louis, MO). Egg SM and 1-acyl-2-[12-[(5-(dimethylamino)-1-naphthalenesulfonyl)amino]dodecanoyl]-*sn*-glycero-3-phosphocholine (DL) were purchased from Avanti Polar Lipids. LDL and cholesterol esterase (CEase) were purchased from Calbiochem. All materials were used as received.

Vesicle Preparation. Stock solutions of each lipid were prepared in chloroform and methanol, and lipid mixtures of desired composition were coprecipitated and subsequently dried under nitrogen using a rotary evaporator. The films were rehydrated in a buffer solution (pH = 6.0) of 0.15 M NaCl and sonicated in the direct mode in an ice bath for 90 min using a Misonix Inc. XL2020 sonicator. An ice−water bath and a nitrogen blanket were used to prevent lipid degradation during sonication, and the resulting bluish dispersions were centrifuged at 20000*g* for 90 min in a Beckman Coulter Allegra64 centrifuge to remove any titanium and unsuspended lipids from the small unilamellar vesicles formed. The supernatant was diluted to a total lipid concentration of 10 mM.

Fluorescence Labeling of LDL. Delivery of fluorophores to LDL was achieved using a slight modification of a procedure described by Smutzer (*19*). Briefly, native LDL was incubated with donor multilamellar vesicles (MLVs) that contained a single fluorophore, followed by centrifugation at 52000*g* for 2 h to isolate the labeled LDL. Incubation conditions were 37 °C, nitrogen atmosphere, and darkness. Delivery of both fluorophores entailed sequential labeling, first with DL followed by DHE. To deliver DL, 2 mL of donor MLVs (0.6 mg/mL) was added to 1 mg of LDL in 4 mL of buffer (0.15 M NaCl). To deliver DHE to unlabeled LDL, 1 mg of LDL in 5 mL was added to 1 mL of donor MLVs (0.21 mg/mL). To assess delivery of individual fluorophores and optimize the labeling protocol, the composition of donor MLVs and the incubation time were varied systematically to assess kinetics and lipid composition profiles. The relative amounts of egg PC, cholesterol, and fluorophore were varied, and it was found that superior delivery was achieved using donor MLVs that did not contain cholesterol. Moreover, the absence of cholesterol in the donor MLVs did not alter significantly the cholesterol-to-phospholipid ratio of the LDL. Accordingly, labeling of LDL with both probes was achieved by first incubating 1 mg of native LDL in 3 mL of buffer with 2 mL of DL donor MLVs (0.6 mg/mL), containing 50 mol % egg PC and the balance DL, for 24 h. After centrifugation, 5 mL of the DL-labeled LDL was further incubated with 1 mL of DHE donor MLVs (0.21 mg/mL) comprising 62.5% egg PC and the balance DHE for 24 h.

Fluorescence and Absorbance Spectroscopy. Quartz cuvettes containing 3 mL of fluorescently labeled vesicles or LDL were exposed to 200 μL aliquots of either buffer (control) or SMase (to induce aggregation). Fluorescence intensities were measured using a PTI, Inc., A-710 steady-state fluorescence spectrometer, and turbidities were measured as absorbance (or optical density) at 450 nm using a Perkin-Elmer BUV40XWO UV−visible absorbance spectrometer. Optical density values were used to correct fluorescence intensities for the inner filter effect according to the equation:

$$F_{corr} = F_{obs} \times 10^{(OD_{ex}+OD_{em})/2} \quad (1)$$

where FI_{obs} is the observed fluorescence intensity, FI_{corr} is the corrected fluorescence intensity, and OD_{ex} and OD_{em} are the optical densities at the excitation and emission wavelengths, respectively.

Dynamic Light Scattering. Particle sizes were analyzed using a Brookhaven 90Plus dynamic light scattering (DLS) apparatus. This system consists of a 15 mW, solid-state laser

operating at a 678 nm wavelength and a BI-9000AT digital autocorrelator. The measured autocorrelation functions were analyzed for the first and second cumulants of a cumulant fit, which provide measures of the apparent diffusivity and the polydispersity, respectively. The data are given in terms of an effective diameter using the Stokes−Einstein equation:

$$\text{effective diameter} = k_B T/3\pi\eta D \qquad (2)$$

where k_B is the Boltzmann constant, T is the temperature (25 °C), η is the solvent viscosity, and D is the diffusivity from the first cumulant.

LDL Compositional Analysis. A full lipid analysis was performed on LDL before and after each labeling step to assess the extent to which the labeling procedure may have altered LDL lipid composition. All lipid analyses were performed as described previously (*20*). Incorporation of fluorescent lipids was verified via fluorescence spectroscopy of native LDL and donor MLVs prior to labeling and of isolated, labeled LDL and spent MLVs after labeling and centrifugation.

Enzymatic Modification. The effect of SMase alone was tested on LDL decorated with both fluorescent probes. The effect of SMase on LDL, which was pretreated with CEase, so as to simulate cholesterol ester hydrolysis, as occurs upon LDL endocytosis by macrophages, was also investigated. Both systems were examined under a fluorescence microscope to detect the first appearance of any cholesterol crystals that might have formed.

Fluorescence Microscopy. Samples were examined daily to inspect for the first appearance of microscopic crystals. Aliquots of 10 μL were mounted on a slide and examined at 1000× magnification using a Zeiss Axioskop2 fluorescent microscope equipped with a Zeiss Axiocam with an Axiovision V2.05 ultraviolet digital imaging system. Three modes of illumination were used, namely, bright field, crossed polarizers, and UV fluorescence with dichroic parameters of excitation of 360 ± 10 nm and emission of 400 nm. Cholesterol crystals were identified as having a platelike habit in bright field as well as appearing birefringent when viewed between crossed polarizers. As native cholesterol is nonfluorescent, the presence of DHE in the sterol crystals was identified qualitatively by UV fluorescence emission.

RESULTS

Fluorescence Assay in LDL-like Vesicles. As a bridge between previous studies involving model hepatic vesicles and intended studies involving native LDL, vesicles were made to resemble LDL by the incorporation of SM such that the outer vesicle bilayer contained a lipid composition resembling that of a plasma LDL monolayer. Such LDL-like vesicles were exposed to SMase and monitored using the DHE-to-DL fluorescence assay for nucleation.

Figure 1 shows the R_F of DHE-to-DL fluorescence intensities as a function of time after SMase addition. As seen with model hepatic vesicles, R_F exhibits a characteristic minimum and increases to and above the initial values within several hours after enzyme addition; crystals are not observed in the microscope until 3 days after enzyme addition. The R_F for a control sample, to which no enzyme was added, exhibits essentially no change other than a modest, but steady, decrease in R_F and yields no crystals.

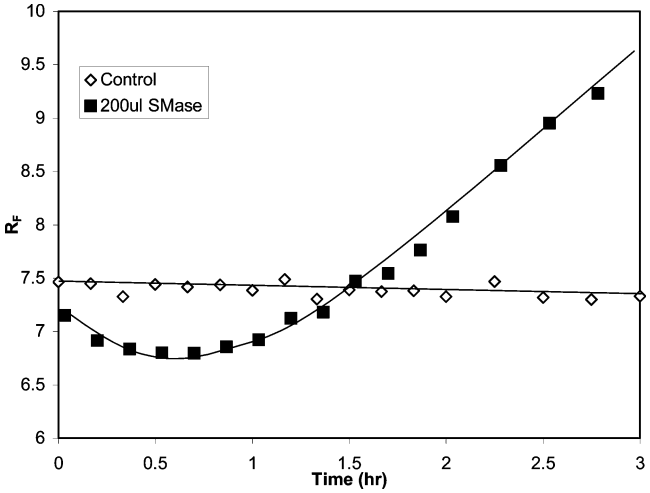

FIGURE 1: SMase-induced cholesterol nucleation in vesicles. Changes in fluorescence spectra are reported in terms of the fluorescence ratio, R_F, which is defined as the DHE fluorescence intensity (at 370 nm) divided by the DL fluorescence intensity (at 467 nm). Excitation was at 300 nm, and the R_F is plotted as a function of time after exposure of fluorescently labeled vesicles to SMase. The vesicle composition was 52% cholesterol, 13% DHE, 16% lecithin, 4% DL, and 15% SM (all percents are mole percents), and the total lipid concentration was 10 mM. No enzyme was added to a control sample (◇), and 10 units of SMase were added to a test sample (■). No change is observed in R_F for the control sample throughout the experiment.

LDL Labeling. Having established a positive response with SMase in vesicles, the next step was to adapt the fluorescence assay to LDL-based systems. Unlike vesicles, which could be synthesized to contain DHE and DL, the fluorophores had to be delivered to existing, native LDL particles. Figure 2 shows the incorporation of DHE and DL into human plasma LDL as a function of time and concentration. Figure 2a reveals that DHE incorporation is rapid, largely finished in 30 min, while DL incorporation proceeds more slowly and reaches saturation after approximately 24 h.

The saturation reached depends largely on the composition of the donor particles. Figure 2b shows the fluorescence spectra of four LDL samples, each measured after 24 h of incubation with a DL-containing donor, each containing a different molar percentage of DL. A dose-dependent response is observed, with a donor containing the largest amount of DL (50 mol %) giving rise to the strongest fluorescence intensity and a donor containing the least amount of DL (7 mol %) giving rise to the weakest fluorescence intensity.

Figure 3 shows the emission spectrum resulting from LDL labeled with both DHE and DL, along with the spectrum of native, unlabeled LDL, and the spectrum of LDL labeled with single fluorophores. Native LDL is essentially nonfluorescent with the exception of a small tryptophan shoulder at about 350 nm, which is suppressed somewhat when LDL is labeled with DL. LDL labeled with DL alone exhibits an emission maximum at about 480 nm, consistent with the spectra of Figure 2b, and labeling LDL with DHE alone produces three fluorescence peaks, at 355, 370, and 393 nm. When both probes are added sequentially to LDL (DL followed by DHE), four emission peaks result, corresponding to the three peaks obtained with DHE alone and the single peak obtained with DL alone. However, the three peaks associated with DHE are less intense in the sample containing both probes than in the sample containing DHE alone.

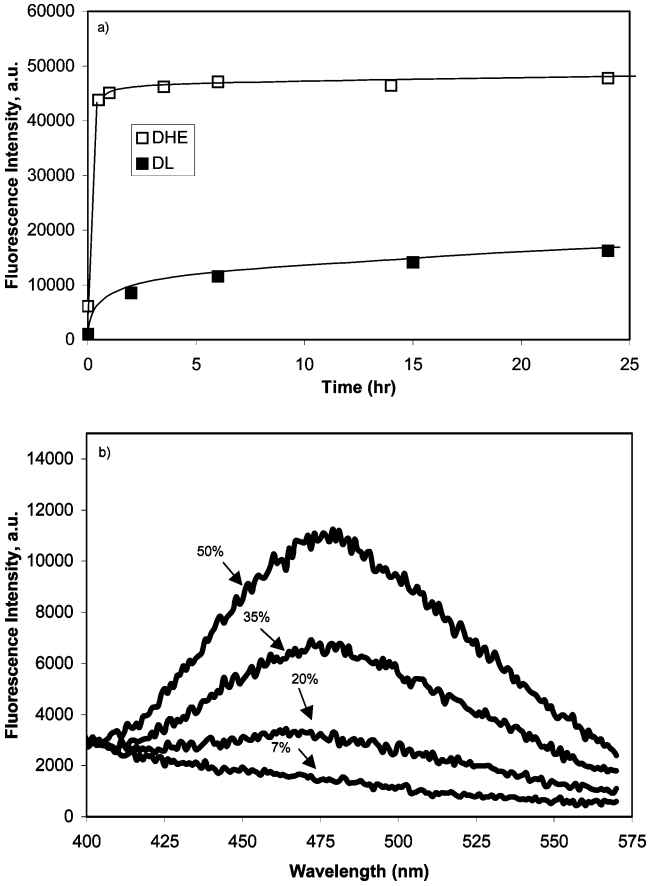

FIGURE 2: Fluorescent labeling of LDL with DL and DHE with exitation set to 300 nm. (a) Labeling of vesicles was performed as described with 1 mg of LDL incubated with 1.2 mg of 50% DL/50% PC MLVs or 0.21 mg of 38% DHE/62% PC MLVs and separated by centrifugation for 2 h at 52000*g*. The fluorescence intensities of LDL labeled with individual fluorophores, DHE (□) and DL (■), increase as a function of incubation time. (b) In a separate experiment, new donor vesicles were made, consisting of DL in the amount shown and the balance PC, and incubated for 24 h with 1 mg of LDL. This labeling proved to be a function of the initial concentration of DL in the donor MLVs. A sequential increase in DL incorporation was observed for increasing concentrations of DL in the donor vesicles.

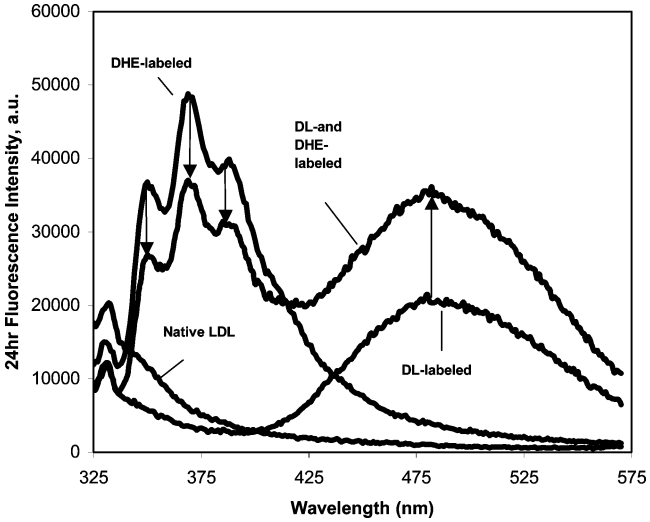

FIGURE 3: Fluorescence emission spectra for four LDL samples after 24 h of incubation with MLVs. Native LDL is essentially nonfluorescent in the wavelengths of the probes when excited at 300 nm. LDL incubated with DL exhibits a characteristic DL peak at about 480 nm, and LDL incubated with DHE exhibits three characteristic DHE peaks at 355, 370, and 393 nm. LDL incubation with DL followed by incubation with DHE exhibits the DL peak at 480 nm and the three DHE peaks. The intensities of DHE and DL in the LDL sample labeled with both fluorophores are less than and greater than, respectively, the intensities in LDL samples labeled with individual fluorophores; this results from DHE-to-DL energy transfer.

Likewise, the DL peak in the sample containing both fluorophores is more intense than in the sample containing DL alone. These results confirm not only the presence of both fluorophores within the LDL, but also the occurrence of DHE-to-DL energy transfer.

Compositional Analysis. Figure 4 shows the total cholesterol-to-phospholipid ratio for LDL before and after incubation with the donor MLVs. Trials 1 and 2 show LDL labeling with only DL MLVs. The before and after cholesterol-to-phospholipid ratios are about the same in these trials. The pellet fraction shows that no cholesterol was transferred from the LDL to the donor particles since the ratio is zero. In trial 3, LDL was labeled with DL alone, DHE alone, and then with both probes sequentially. In each case, the initial and final total cholesterol-to-phospholipid ratios were about the same.

Aggregation Studies. LDL containing both fluorophores were then used to examine the response of LDL to various combinations of enzymes known to be important in atherosclerosis. SMase-induced aggregation was quantified using a combination of turbidity, measured as absorbance at 450 nm, and dynamic light scattering. Two populations of labeled LDL were used, one of which had no prior treatment (other than fluorescence labeling) and one that had been exposed to CEase for 24 h. Figure 5 shows that the aggregation behavior of the two LDL populations is drastically different. Whereas fluorescently labeled, but otherwise native, LDL does exhibit some evidence of aggregation, regardless of SMase concentration, LDL which had been pretreated with CEase exhibits significant aggregation, in a dose-dependent fashion, in response to SMase.

Figure 6 provides additional insights into the aggregation process and shows light-scattering-intensity-weighted size distributions as function of time after SMase addition for an LDL sample that had been pretreated with CEase. Initially, the LDL size distribution is largely monodisperse and centered at approximately 20 nm, in good agreement with the known size range of LDL in vivo. Three hours after SMase addition, the distribution becomes much more polydisperse and appears bimodal; one mode spans a size range similar to that seen with the initial particle population of monomeric LDL, but the distribution is dominated by a second mode of larger particles in the size range 47−200 nm. Consistent with this is an increase in the effective diameter from 20.9 nm initially to 78.1 nm after 3 h. Eight hours after enzyme addition, the size distribution again appears unimodal but not monodisperse. The relative fractions of particles greater than 100 nm increase, as does the effective diameter (to 96.1 nm).

Fluorescence Assay in Labeled LDL. The DHE-to-DL energy transfer assay was used to quantify the LDL response to both CEase and SMase, and Figure 7 shows temporal changes in fluorescence intensity of both DHE (Figure 7a) and DL (Figure 7b). Results of four LDL samples are shown: a control sample, to which neither enzyme was

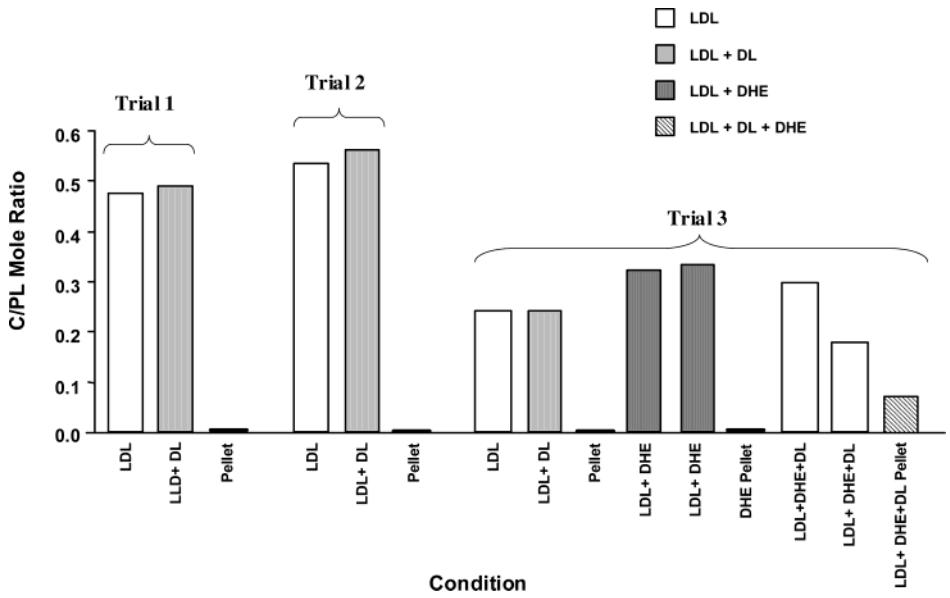

FIGURE 4: LDL compositional analysis. Compositional analysis for LDL before and after labeling showed little change, if any, in the total cholesterol-to-phospholipid ratio. In trials 1 and 2, LDL was labeled with DL MLVs only. The pellet fractions show that the donor particles have a value of about zero since no cholesterol was transferred to them from the LDL. In the third trial, LDL was labeled with DHE alone and then with DL followed by DHE. Again, little change in the total cholesterol-to-phospholipid ratio is observed.

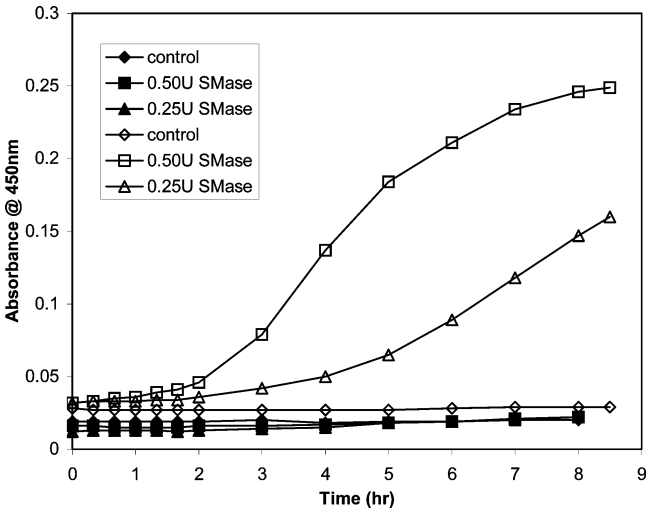

FIGURE 5: CEase- and SMase-induced aggregation of labeled LDL. LDL labeled with both DHE and DL was divided into six aliquots (two groups of three aliquots). One group was incubated with the enzyme, cholesterol esterase, at a level of 0.5 unit of enzyme per mg of LDL lipid, and another group was left untreated. SMase was added to both groups with the CEase group getting no SMase as a control (◇), 0.25 unit (△), and 0.5 unit (□). The group with no CEase received no SMase as a control (♦), 0.25 unit (▲), and 0.5 unit (■) SMase. Aggregation, measured as absorbance at 450 nm, was observed. The absorbance for the samples pretreated with CEase exhibit roughly a 5-fold increase than the samples treated with SMase alone.

added, and three samples to which both CEase and SMase were added. The CEase concentration in the latter three samples was fixed at 5 units, and different amounts of SMase were added 2 h after CEase addition as shown in Figure 7.

The addition of CEase induces an apparent enhancement of energy transfer within 30 min, as evidenced by a decrease in DHE intensity and a concomitant increase in DL intensity. No such changes are observed in the control without CEase. From 30 min until 2 h after CEase addition, the fluorescence intensity of both fluorophores remains essentially constant. Following the 2 h CEase incubation period, the DHE fluorescence intensity increases steadily, and the DL intensity decreases concomitantly, in a dose-dependent fashion with the addition of varying amounts of SMase. Within an hour after SMase addition and after a significant decrease, the DL intensity subsequently increased in the sample with the highest SMase loading.

These changes in fluorescence are quantified in terms of the fluorescence ratio, which is plotted as a function of time in Figure 8. The control sample exhibits no change in R_F, but R_F correlates with SMase for three samples to which this pronucleating enzyme was added. Specifically, R_F increases from 0.06 at 2 h to 0.07, 0.11, and 0.12 at 3.2 h for SMase loadings of 0.25, 1.0, and 5.0 units, respectively. Whereas R_F begins to plateau at this time point in the sample with the highest SMase concentration (owing to the rise in DL intensity, which offsets the rise in DHE intensity), R_F continues to increase in a dose-dependent fashion for the other two SMase samples. The sample containing the highest SMase loading was the only one observed to yield crystals, which first appeared in the fluorescence microscope 24 h after SMase addition. Figure 9 shows a fluorescence microscope image of these early crystals; bright areas are regions of UV fluorescence owing to the presence of DHE.

DISCUSSION

DHE-to-DL resonance energy transfer has been used to study vesicle-to-micelle transitions, sterol flip-flop in biological membranes, and nanodomain formation in lipid bilayers (*8*), as well as bile salt- and PLC-induced nucleation of cholesterol crystals (*12*, *13*). Important to this work is the fact that the characteristic minimum in R_F observed in PLC systems has been determined, unequivocally, to be a result of two competing events. The initial decrease in R_F stems from an increase in DL intensity that arises because of cleavage of polar phosphocholine headgroups by PLC. The reason for the increase is that the dansyl moiety is itself polar; the removal of polar headgroups surrounding dansyl decreases the dansyl Stokes shift with a concomitant increase

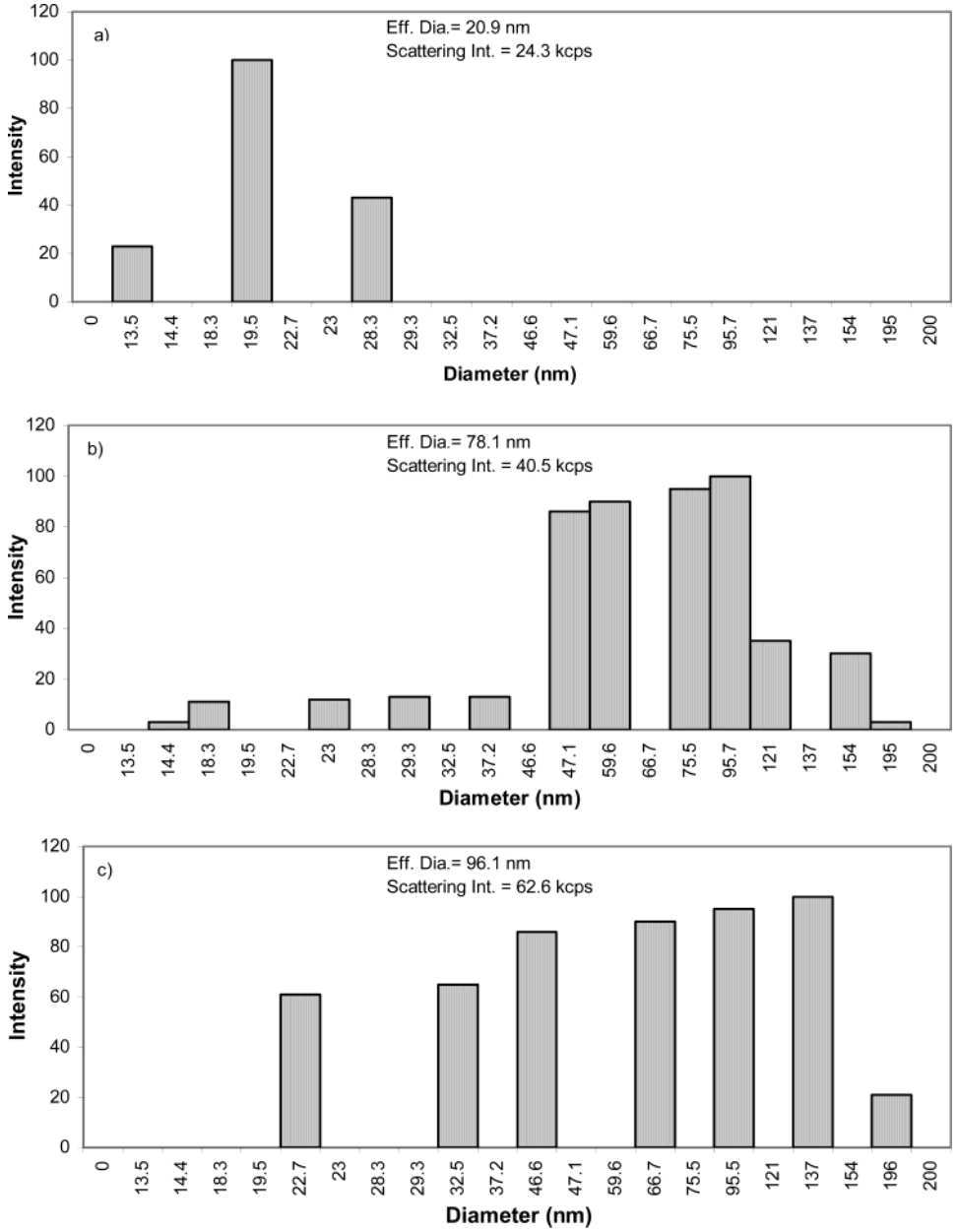

FIGURE 6: Labeled LDL was analyzed using DLS to track particle size during the course of enzyme action. Five units of CEase was added to 0.5 mg of LDL in 3 mL. After 1 h 0.25 unit of SMase was added to the sample. Initially after SMase addition, (a) the particle sizes were centered around 20.9 nm, but after 3 h (b) the effective diameter had increased to 78.1 nm, and after 8 h (c) the distribution and size had increased further to 96.1 nm. As the aggregates become larger, the light scattering increases.

in quantum yield. The subsequent increase in R_F stems from an alleviation of energy transfer, owing to removal of DHE, but not DL, from the vesicle bilayer into a sterol crystalline phase. The minimum in R_F signifies the point in time at which the kinetics of nucleation dominate the kinetics of enzyme hydrolysis.

In view of this, the R_F profile observed for SM-containing vesicles upon exposure to SMase (Figure 1) is easily understood. As SMase cleaves polar phosphocholine headgroups, in a fashion similar to PLC, the DL intensity increases. At short times (that is, prior to nucleation), there is essentially no change in the DHE intensity, so the net effect is a decrease in R_F. As nucleation proceeds, DHE-to-DL energy transfer is alleviated, causing R_F to increase to and above the initial value. The similarities observed among the two enzyme/vesicle systems further reinforce the versatility of the DHE−DL FRET assay and lend credibility to its adaptation to blood-based systems.

A challenge in adapting the assay to blood-based systems is the incorporation of the fluorescent probes into the particles of interest. Whereas model vesicles can be easily synthesized to mimic hepatic vesicles found in vivo, and hence DHE and DL can be added to model vesicles during synthesis, synthesis of model LDL is intractable. Hence, studies involving LDL must be done with native particles, necessitating that DHE and DL be delivered to an existing particle. This was achieved by incubation of donor liposomes with native LDL, followed by centrifugation to isolate labeled LDL. Shuttling agents (e.g., cyclodextrins to deliver DHE and phospholipid transfer protein to deliver DL) proved to be unnecessary; in fact, use of the former has been shown to significantly alter the native Chol-to-phospholipid ratio

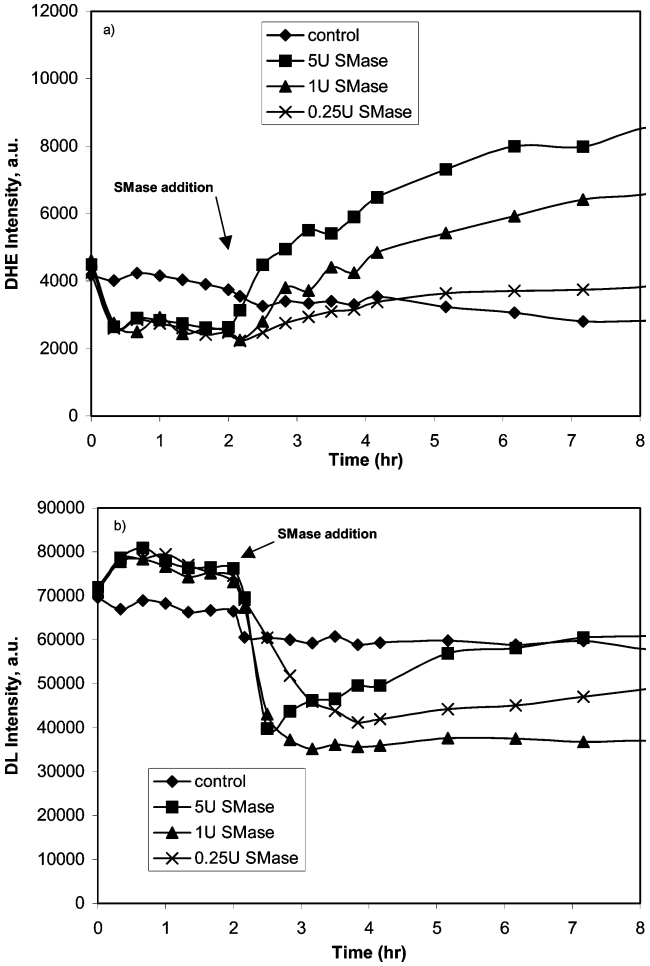

FIGURE 7: Fluorescence energy transfer from DHE to DL in LDL. Five units of CEase were added to 3 mL aliquots of fluorescently labeled LDL. CEase contributed 2200 intensity units, which were subtracted out of the readings. After 2 h, SMase was added to the samples in the following amounts: none was added to a control sample (◆), 0.25 unit (×), 1 unit (▲), and 5 units (■). (a) The DHE intensity initially decreased, followed by an increase after SMase addition in a dose-dependent manner. (b) The DL intensity initially increased, but after SMase addition the intensity dramatically decreased. The decrease was initially dose-dependent, but 30 min after SMase addition, the sample with the highest loading began to increase.

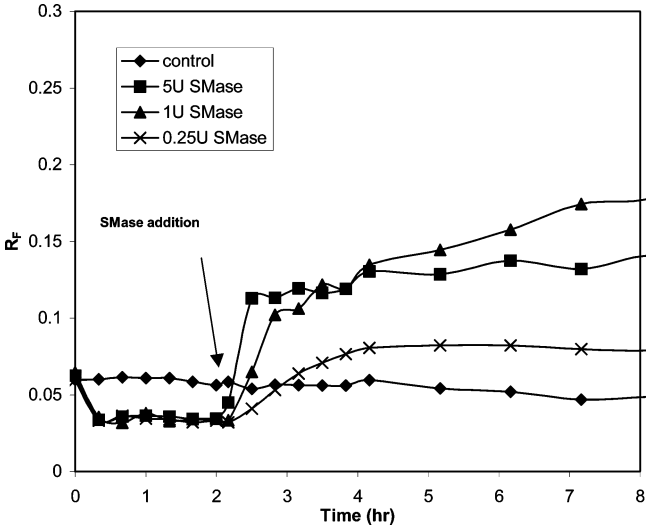

FIGURE 8: Fluorescence ratio for CEase- and SMase-treated LDL. The fluorescence ratio, R_F, increased after SMase addition because of the alleviation of energy transfer signifying cholesterol nucleation in the group pretreated with CEase. The SMase loadings were as in Figure 6: none was added to a control sample (◆), 0.25 unit (×), 1 unit (▲), and 5 units (■). Crystals were first observed after 24 h in the 5 unit SMase sample, and no crystals were observed in the control sample.

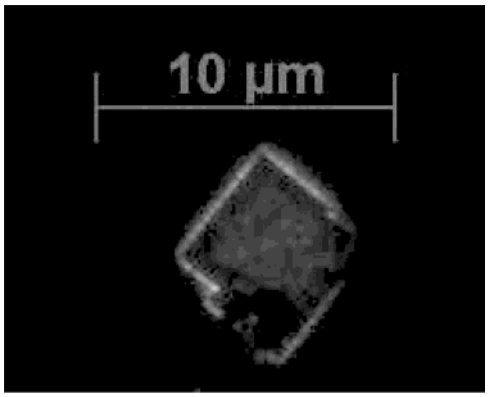

FIGURE 9: Fluorescent cholesterol crystal. First visible evidence of a cholesterol crystal seen under fluorescent light microscope 24 h after CEase-pretreated LDL exposure to 5 units of SMase. The crystal fluoresces due to conucleation of DHE with cholesterol.

of parent LDL. Such was not the case with the incubation protocol used herein where the cholesterol-to-phospholipid ratio shows little change after incubation with donor particles (Figure 4).

Several lines of evidence indicate successful labeling of LDL with DHE and DL. First, native LDL is nonfluorescent in the spectral region 375−575 nm, whereas LDL fractions obtained after labeling exhibit significant fluorescence intensity and emission maxima that are characteristic of DHE and DL.

Second, the DL emission maximum, which occurs at 512 nm in (sterol-free and hence relatively more polar) donor vesicles, shifts to 480 nm in the (cholesterol-containing and hence relatively less polar) LDL fraction after labeling. This indicates that DL is residing in a less polar environment, as would be expected in an LDL, cholesterol-containing monolayer. The emission maximum of DL is known to shift from 512 nm in (cholesterol-free) PC−DL vesicles to 470 nm in PC−Chol−DL vesicles containing 60% cholesterol (*8*).

Third, the fluorescence intensity of DL in the LDL fraction obtained after labeling correlates, in a dose-dependent fashion, with the DL content of the donor liposomes (Figure 2b). A similar dose-dependent response is observed with DHE (data not shown). Moreover, the fluorescence intensities in the LDL fractions after labeling increased with time for a given fluorophore content in the donor liposomes.

Fourth, and perhaps most convincing, sequential labeling with both fluorophores led to an emission spectrum containing four spectral peaks, three of which are characteristic of DHE and one of which is typical of DL. Comparing fluorescence intensities in LDL fractions comprising both fluorophores with those comprising individual fluorophores reveals that the DHE intensity is less intense, whereas the DL intensity is more intense, in the latter. This is very strong evidence not only that DHE was successfully incorporated into LDL that had been previously labeled with DL but that the DL derived additional fluorescence as a result of energy transfer from DHE.[2]

Having established successful labeling of LDL with DHE and DL, the DHE-to-DL FRET assay was used, along with light scattering and absorbance spectroscopy, to quantify alterations to LDL caused by SMase and CEase. The primary modification to LDL upon exposure to SMase is particle aggregation. The extent of aggregation depends on the relative amount of LDL to SMase, and SMase-induced aggregation was modest at the concentrations utilized herein. This is evident from the small increase in absorbance (Figure 5) for samples exposed only to the enzyme SMase. Even though there is LDL aggregation after SMase addition, this aggregation does not induce cholesterol crystal formation. The extent of LDL aggregation, for a particular SMase concentration, can be increased significantly if LDL is previously exposed to the enzyme CEase.

This combined effect of CEase and SMase is shown clearly in Figure 5, where the same SMase loadings that yield very modest LDL aggregation in the absence of CEase produce significantly higher levels of aggregation in LDL samples which had been incubated previously with CEase. The SM concentration, which is identical in each sample, is calculated based on the concentration of LDL used, the lipid concentrations stated by the distributor (Calbiochem), and the published composition of LDL (*21*). In Figures 5−8, the SM concentration is approximately 0.016 mg/mL, both in the presence and in the absence of CEase, as CEase does not affect the SM concentration, but rather the concentrations of cholesterol ester and free cholesterol. The ceramide formed from SMase action is known to form ceramide-rich domains in the monolayer and can also partition into the core (*22*, *23*). The presence of cholesterol will enhance the ability of ceramide to form domains in the monolayer as well as the formation of cholesterol-rich domains (*24*). These ceramide-rich patches facilitate LDL aggregation.

Treatment of LDL with CEase changes the distribution of molecules between the surface and the core, with the main result being the incorporation of more free cholesterol into the monolayer (*25*, *26*). Another consequence of treatment with CEase is a partitioning of DHE into the LDL core, in response to CEase-induced compositional and enthalpic changes to the LDL particle (*27*). The resulting decrease in hydrophobicity within the LDL core potentially favors a microstructural transition to liposome structures. Moreover, the increase in cholesterol in the LDL monolayer favors LDL aggregation, typically on a time scale of days. While it is clear that CEase induces LDL aggregation for these reasons, it has been shown that LDL aggregation requires CEase activities above 15 units/mL (*25*). Here, the highest activity of CEase used was just 1.67 units/mL. Moreover, the time of incubation with CEase (2 h) was far less than the time required to observe cholesterol-induced aggregation. This explains the apparent lack of aggregation observed with CEase alone.

The dynamic light scattering results of Figure 6 show that the increase in turbidity observed in the presence of both enzymes results from LDL particle aggregation, rather than mere growth. Not only does the distribution broaden with time, but the distribution also becomes multimodal, with one of the modes corresponding to the size of initial LDL particles. Growth of particles would cause the initial size distribution to shift toward larger sizes, with little change in polydispersity, and cause the initial mode to disappear. The continued presence of the initial mode indicates that the larger particles observed are a result of aggregation and not growth.

LDL aggregation is not the only effect produced by the combined action of CEase and SMase. Whereas neither enzyme alone produces cholesterol nucleation, the concerted action of the two enzymes yields visible (in the microscope) cholesterol crystals within a day. Again, this likely relates to the conversion of esterified cholesterol within the LDL core to free cholesterol, which increases the level of cholesterol saturation. Native LDL is undersaturated in free cholesterol and therefore cannot nucleate cholesterol crystals even upon SMase-induced aggregation; however, LDL treated with CEase can become supersaturated so that cholesterol crystals are expected as an equilibrium thermodynamic phase.

Supersaturation, though, does not guarantee crystallization. For example, liposomes that are supersaturated with cholesterol are well-known to be metastable and "long-lived" for periods of months. Cholesterol−lecithin vesicles do not nucleate cholesterol crystals, regardless of the cholesterol content, prior to aggregation. CEase-treated LDL appears to also be kinetically stabilized in a similar fashion. Thus, the addition of SMase, which facilitates LDL aggregation, also facilitates nucleation of cholesterol crystals.

These effects are quantified by the DHE-to-DL FRET assay, which reveals that incubation with CEase alone is insufficient to produce nucleation and that nucleation commences very soon after the subsequent addition of SMase. Examination of harvested crystals, which fluoresce under a fluorescence microscope (Figure 9), confirms that the observed alleviation of energy transfer, and hence the upturn in R_F (Figure 8), results from cholesterol nucleation. As cholesterol is nonfluorescent, the fact that these crystals fluoresce can only be explained by the presence of DHE within the crystal. The partitioning of DHE into the crystalline phase accounts for the loss of energy transfer from DHE to DL.

The upturn in DL intensity (Figure 7b) is the result of competing effects. The initial drop is a result of the loss of energy transfer from DHE to DL as DHE leaves the monolayer. This is explained by the simultaneous rise in DHE intensity (Figure 7a). SMase treatment alone on labeled LDL results in a rise in the DL intensity with an eventual plateau in intensity (results not shown). This is a result of the decrease in polarity of the monolayer as the enzyme cleaves the polar headgroup of SM. This is also the case in CEase-pretreated LDL after SMase exposure. Here the loss of energy transfer dominates at short times followed by the increase in DL intensity at longer times due to a decrease in membrane polarity.

These results hold potentially important insights into the mechanism of cholesterol crystal formation during athero-

[2] Strictly speaking, energy transfer also occurs from the tryptophan residue in the protein (apo B-100) of LDL to DL. This is evident by a decrease in intensity of the shoulder at 350 nm between the native LDL emission curve and the DL-labeled curve. As the excitation in this work is 300 nm, whereas maximal tryptophan absorbance is at 280 nm, the relative amount of tryptophan-to-DL energy transfer is small and does not affect the changes in DHE-to-DL energy transfer that arise because of enzyme hydrolysis and nucleation.

sclerosis. It is currently unknown whether crystals originate directly from LDL within the extracellular space or intracellularly after uptake of modified LDL by macrophages, or both. These in vitro studies point to a likely role for cellular uptake prior to nucleation. Native LDL certainly does not nucleate cholesterol crystals directly. In our hands, enzymatic modification of LDL by SMase alone results in aggregation but not nucleation. The aggregation stems from generation of ceramide on the LDL monolayer and an unfavorable exposure of hydrophobic ceramide regions to water. Such aggregation does not yield nucleation because it has done nothing to change the level of free cholesterol, which is less than saturation.

Also in our hands, enzymatic modification by CEase alone does not produce aggregation, nucleation, or crystallization. The effect of CEase is to increase the level of free cholesterol, to and above the level of saturation. However, even LDL that is supersaturated with cholesterol as a result of CEase action does not necessarily yield cholesterol crystals. Here the kinetics and mechanism of nucleation become important. It appears that formation of a critical cholesterol cluster requires a pooling of cholesterol from multiple LDL particles. Before cholesterol can nucleate from LDL, the LDL must first aggregate.

This accounts for the synergistic effect of CEase and SMase. CEase raises the level of cholesterol saturation to the point where crystals are expected as an equilibrium phase, and SMase induces aggregation of LDL so that cholesterol nuclei can form. SMase is, without question, an extracellular enzyme. There is some evidence to suggest that CEase is present in artery walls and can be released into the circulation (*25*). Thus, strictly speaking, our results cannot negate unequivocally the possibility that crystals develop in the extracellular space. However, CEase is primarily found in macrophages where it is associated with the cholesterol ester cycle. Any synergistic action of SMase and CEase in vivo most likely involves macrophages so that nucleation of cholesterol crystals proceeds in the intracellular space.

REFERENCES

1. Small, D. (1988) Progression and Regression of Atherosclerotic Lesions. Insights from Lipid Physical Biochemistry, *Arteriosclerosis 8*, 103−129.
2. Kellner-Weibel, G., Yancy, P. G., Jerome, W. G., Walser, T., Mason, R. P., Phillips, M. C., and Rothblat, G. H. (1999) Crystallization of free cholesterol in model macrophage foam cells, *Arterioscler. Thromb. Vasc. Biol. 19*, 1891−1898.
3. Fuster, V., Badimon, L., Badimon, J., and Cheesebro, J. H. (1992) The pathogenesis of coronary artery disease and the acute coronary syndromes, *N. Engl. J. Med. 326*, 242−250, 310−318.
4. Felton, C. V., Cook, D., Davies, M. J., and Oliver, M. F. (1997) Relation of plaque lipid composition and morphology to the stability of human aortic plaques, *Arterioscler. Thromb. Vasc. Biol. 17*, 1337−1345.
5. Schroeder, A. P., and Falk, E. (1995) Vulnerable and dangerous coronary plaques, *Atherosclerosis, Suppl. 118*, S141−S149.
6. Tangirala, R. K., Jerome, W. G., Jones, N. L., Small, D. M., Johnson, W. J., Glick, J. M., Mahlberg, F. H., and Rothblat, G. H. (1994) Formation of cholesterol monohydrate crystals in macrophage-derived foam cells, *J. Lipid Res. 35*, 93−104.
7. Guyton, J. R., and Klemp, K. F. (1989) The lipid-rich core region of human atherosclerotic fibrous plaques, *Am. J. Pathol. 134*, 705−717.
8. Troup, G., Tulenko, T. N., Lee, S. P., and Wrenn, S. P. (2003) Detection and Characterization of Cholesterol Domains in Biological Membranes, *Colloids Surf., B 29*, 217−231.
9. Huang, J., Buboltz, and Feigenson, G. (1999) Maximum solubility of cholesterol in phosphatidylcholine and phosphatidylethanolamine bilayers, *Biochim. Biophys. Acta 1417*, 89−100.
10. Stryer, L. (1978) Fluorescence energy transfer as a spectroscopic ruler, *Annu. Rev. Biochem. 47*, 819−846.
11. Kim, Y. S., Luk, A. S., Kaler, E. W., and Lee, S. P. (1994) *Gastroenterology 106*, A343 (Abstract).
12. Wrenn, S. P., Lee, S. P., and Kaler, E. W. (1999) A fluorescence energy transfer study of lecithin-cholesterol vesicles in the presence of phospholipase C, *J. Lipid Res. 40*, 1483−1494.
13. Wrenn, S. P., Gudheti, M., Veleva, A. N., Lee, S. P., and Kaler, E. W. (2001) Characterization of Model Bile Using Fluorescence Energy Transfer from Dehydroergosterol to Dansylated Lecithin, *J. Lipid Res. 42*, 923−934.
14. Tulenko, T. N., Chen, M., Mason, P. E., and Mason, R. P. (1998) Physical effects of cholesterol on arterial smooth muscle membranes: evidence of immiscible cholesterol domains and alterations in bilayer width during atherogensis, *J. Lipid Res. 39*, 947−956.
15. John, K., Kubelt, J., Müller, P. O., Wüstner, D., and Hermann, A. (2002) Rapid Transbilayer Movement of the Fluorescent Sterol Dehydroergosterol in Lipid Membranes, *Biophys. J. 83*, 1525−1534.
16. Williams, K. J., and Tabas, I. (1995) The response-to-retention hypothesis of early atherogensis, *Arterioscler. Thromb. Vasc. Biol. 15*, 551−561.
17. Williams, K. J., and Tabas, I. (1998) The response-to-retention hypothesis of atherogensis reinforced, *Curr. Opin. Lipidol. 9*, 471−474.
18. Li, F., and Hui, D. Y. (1997) Modified low-density lipoprotein enhances the secretion of bile salt-stimulated cholesterol esterase by human monocyte-macrophages, *J. Biol. Chem. 272*, 28666−28671.
19. Smutzer, G. (1988) A fluorescent sterol probe study of human serum low-density lipoproteins, *Biochim. Biophys. Acta 958, 323−333*.
20. Chen, M., Mason, R. P., and Tulenko, T. N. (1995) Atherosclerosis alters the composition, structure and function of arterial smooth muscle cell plasma membranes, *Biochim. Biophys. Acta 1272*, 101−112.
21. Hevonoja, T., Pentikäinen, M. O., Hyvönen, M. T., Kovanen, P. T., and Ala-Korpela, M. (2000) Structure of low-density lipoprotein (LDL) particles: basis for understanding molecular changes in modified LDL, *Biochim. Biophys. Acta 1488*, 189−210.
22. Ohta, N., and Hatta, I. (2002) Interaction among molecules in mixtures of ceramide/stearic acid, ceramide/cholesterol and ceramide/stearic acid/cholesterol, *Chem. Phys. Lipids 115*, 93−105.
23. Carrer, D. C., Härtel, S., Mónaco, H. L., and Maggio, B. (2003) Ceramide modulates the lipid membrane organization at molecular and supramolecular levels, *Chem. Phys. Lipids 122*, 147−152.
24. Sparr, E., Eriksson, L., Bouwstra, J. A., and Ekelund, K. (2000) AFM Study of Lipid Monolayers: III. Phase Behavior of Ceramides, Cholesterol and Fatty Acids, *Langmuir 17*, 164−172.
25. Aviram, M., Keidar, S., Rosenblat, M., and Brook, G. J. (1991) Reduced uptake of cholesterol esterase-modified low-density lipoprotein by macrophages, *J. Biol. Chem. 266*, 11567−11574.
26. Oörni, K., Pentikäinen, M. O., Ala-Korpela, M., and Kovanen, P. T. (2000) Aggregation, fusion, and vesicle formation of modified low-density lipoprotein particles: molecular mechanisms and effects on matrix interactions, *J. Lipid Res. 41*, 1703−1714.
27. Li, Q. T., and Sawyer, W. H. (1993) Effect of cholesteryl ester on the distribution of fluorescent cholesterol analogues in triacylglycerol-rich emulsions, *Biochim. Biophys. Acta 1166*, 145−153.

BI035747R